Journal of Engg. Research Vol. 7 No. (4) December 2019 pp. 37-57

Numerical study of seismic response of trapezoidal alluvial valleys against vertically propagating incident waves

Mohammad Hossein Taghizadeh Valdi*, Mohammad Reza Atrechian**, Ata Jafary Shalkoohy*** and Ali Tighnavard Balasbaneh****

**Department of Civil Engineering, Isfahan (Khorasgan) Branch, Islamic Azad University, Isfahan, Iran*
***Department of Civil Engineering, Zanjan Branch, Islamic Azad University, Zanjan, Iran*
****Department of Civil Engineering, Bandar Anzali Branch, Islamic Azad University, Bandar Anzali, Iran*
*****Structure and Materials Department, School of Civil Engineering, Faculty of Civil Engineering, Universiti Teknologi Malaysia, Malaysia*
**Corresponding Author: mh.taghizadeh@khuisf.ac.ir*

ABSTRACT

The experience of previous earthquakes in the world shows that the structural damage due to the earthquakes is highly influenced by the site condition, which is known as site effects. Since most cities are built on alluviums, studying the seismic response of alluvial basin, which are the site of many structures, is very important. This study investigates the seismic response of 2D trapezoidal alluvial valleys with slope angles of 31°, 45°, and 71.5°, against P and SV vertically propagating incident waves in middle and lateral areas of the valleys. Then the effect of changes in Poisson's ratio and specific weight of alluvial materials on the seismic response of the valley in the mentioned areas is investigated. Numerical modeling is done using QUAKE/W finite element software, based on the equivalent linear analysis. According to the results, by increasing the slope angle of the valley, the vertical acceleration and displacement response spectrum in the middle and lateral areas of the alluvial valley decrease and increase, respectively. Moreover, by increasing the Poisson's ratio and specific weight of alluvial materials, the vertical acceleration and displacement response spectrum in the middle area of the valley decrease, but do not undergo tangible changes in the lateral areas of the valley.

Keywords: Site effects; trapezoidal alluvial valleys; slope angle; finite element method.

INTRODUCTION

Rivers wash the earth's crust on their path and these washed materials are carried by the fast water flow till they reach a low slope region of the ground and as a result, they remain in the same region and are deposited. These deposited materials create a fertile soil, which is called alluvium. Alluvium is typically composed of fine particles and materials of mud, clay, and coarse particles of sand and gravel. Now, if these materials are deposited in the gap between the two mountains (so called valley), they create alluvial valleys. Most of the cities are located on the basin, in which these valleys are samples of the subsurface natural phenomenon and there is always the possibility of an earthquake occurring in these areas; hence, seismic studies of alluvial areas are the most important topics in geology and geotechnical engineering. The obtained results indicate that, in wide valleys with low depth, one-dimensional evaluation of the site is a good estimation of the seismic motion of the earth in the middle area of alluvial valley, but in its lateral areas, the one-dimensional analysis leads to cautious results. On the other hand, in narrow deep valleys, the one-dimensional analysis in the lateral areas of the valley leads to conservative results, while for the higher frequencies in the middle area of the valley results are underestimated. About 50 years ago, earthquakes are divided into two categories of near-field and far-field earthquakes based on the distance between the registration point of the record and the fault. The first near-field earthquake was reported by Benioff in 1955, which was related to Kern

County earthquake of California in 1952. Benioff (1955) showed that energy release due to fault fraction can create two different types of shakes in two ends of the fraction area. Subsequently, two other well-known earthquakes of Parkfield (1966) and San Fernando (1971) occurred, which can be considered as the basis of studies regarding the near the fault earthquakes. Among the recent earthquakes, Northridge (USA, 1994), Kobe (Japan, 1995), Izmit (Turkey, 1999), and Chi-Chi (Taiwan, 1999) earthquakes can be considered as the most important and the most devastating near-field earthquakes. Investigating the severity of destruction due to earthquakes in the last decade highlighted the importance of site effects and surface geological conditions. Most of the recent devastating earthquakes in Iran and other countries of the world illustrated the great importance of site effects. In many of the site effects related studies based on the numerical analysis of alluvium, a part of underground layers is taken into account, which enhances seismic motion. This part is located on a layer with high resistance properties, which do not amplify the earthquake induced waves, and is called seismic bedrock. The existence of alluvial substrates in different regions of Iran including alluvial regions of the north, metamorphic deposits of the southern margins of Iranian Plateau, and alluvial substrates of cities such as Tehran, Isfahan, Qom and Kermanshah, etc. Led to the importance of investigating their seismic behavior. Bouchon (1973) was the first researcher to investigate the effect of semi-sine hills on the seismic response of the earth surface. Although he considered various shape ratios in his studies, the results presented were only related to SH incident waves. Later, Geli et al. (1988) investigated the subsurface layers and the existence of adjacent nonsmooth regions on seismic response of semi-sine hills. But their field of studies was just limited to SH incident wave and ultimately to one-shape ratio. Sanchez-Sesma (1987) was the first researcher to examine the seismic behavior of sharp-cornered hills. His field of study just included triangular shaped hills, SH incident wave, and a specific Poisson's ratio. Sanchez-Sesma & Campillo (1991, 1993) were the first group to investigate the effect of semi-elliptical hills on seismic response of the earth's surface. Although they examined both SV and P body waves, the field of their studies only included one shape ratio and Poisson's ratio. Later, Pedersen et al. (1994) considered different incident and azimuth angles in studying seismic response of 2D semi-elliptical hills, but their field of study was still limited to one shape ratio and Poisson's ratio. Moczo et al. (1997) studied the seismic response of trapezoidal hills. Their field of study also included SV incident wave, one shape ratio, angle of slope, and Poisson's ratio. Kamalian et al. were the first group to perform extensive parametric studies to investigate the seismic behavior of trapezoidal hills (2004), semi-elliptical (2004), and semi-sine (2006) against SV and P vertically incident waves. In their studies, which were conducted using finite element method, the effect of shape ratio, the ratio of incident wave length to dimensions of the phenomenon, angle of slope (in trapezoidal hills), and Poisson's ratio on seismic response of the mentioned hills were examined separately. This paper presents the results of a numerical parametric study on the seismic response of 2D trapezoidal alluvial valleys with slope angles of 31^{o}, 45^{o}, and 71.5^{o} against P and SV vertically propagating incident waves, using finite element method (FEM). Then by changing Poisson's ratio and specific weight of the alluvial materials of the trapezoidal valley with slope angles of 45^{o}, its seismic response will be investigated in its middle and lateral areas. The numerical modeling is performed using QUAKE/W finite element software based on dynamic analysis of linear equation. The parameters under study include vertical displacement and acceleration values and comparing their response spectrum in middle and lateral areas of the valleys.

INTRODUCTION OF QUAKE/W

In the present study, the numerical modeling of the alluvial valleys was performed using the QUAKE/W finite element software, based on the equivalent linear analysis. Quake/w is a geotechnical finite element software product for the dynamic analysis of earth structures subjected to earthquake shaking, or point dynamic forces from a blast, or a sudden impact load. It determines the motion and excess pore-water pressures that arise due to shaking. Its comprehensive formulation makes Quake/w well suited for analyzing a wide range of problems. Generalized material property functions allow us to use any laboratory or published data. Three constitutive models are supported: a linear elastic model, an equivalent linear model, and an effective stress nonlinear model. Quake/w uses the direct integration method to compute the motion and excess pore-water pressures arising from inertial forces at user-defined time steps. The response and behavior of earth structures subjected to earthquake shaking are highly complex and multifaceted. Generally, there are the following issues (Bararpour et al., 2016):

- The motion, movement, and inertial forces that occur during the shaking.
- The generation of excess pore-water pressures.
- The potential reduction of the soil shear strength.
- The effect on the stability of the inertial forces, excess pore-water pressures, and possible shear strength loses.
- The redistribution of excess pore-water pressures and possible strain softening of the soil after the shaking has stopped.
- The permanent deformation, which sometimes may be tolerable but can also be very large and cause severe damage when there is extensive liquefaction.

QUAKE/W (Geo-Slope Office, 2012) has been implemented using dynamic memory allocation, so there is no specific limit on problem size in terms of number of nodes, element or material types. Therefore, the maximum size of the problem is a function of the amount of available computer memory. Isoparametric quadrilateral and triangular finite elements can be implemented and each may have various numbers of optional secondary nodes to provide higher order interpolation of nodal values within the element. When QUAKE/W performs an Equivalent Linear analysis (EQL), the Damping Ratio and G modulus vary with cyclic strain for successive iterations. The equivalent linear model can be considered as non-linear, but it is equivalent to a linear model because it transforms the irregular earthquake shaking into equivalent uniform cycles. It is non-linear in that the shear modulus G is modified (reduced) in response to cyclic shear strains. Each iteration is linear (i.e., G is a constant), but the modification of G after each iteration makes the analysis non-linear. Equivalent linear analysis is based on total stresses and the effects of seismically induced pore-water pressure on strength and stiffness cannot be taken into account continuously during the analysis. In addition, since the analysis is elastic, it can be used to compute permanent deformation of slopes by one of the two approaches. The first approach uses acceleration output from the analysis and the second uses the cyclic shear stress output. These procedures appear to work quite well provided the behavior of the structure is not strongly non-linear and significant pore pressure does not develop.

METHODOLOGY OF PARAMETRIC ANALYSIS

The aim of solving this problem is the ability of the finite element method in the dynamic analysis of the seismic response of alluvial valleys with different angles and to investigate the effects of the changes in Poisson's ratio and impedance of materials on the seismic response of alluvial valleys. Figure 1 illustrates the computational field, boundary conditions, and geometric dimensions of the numerical solution environment. Numerical modeling includes 2D trapezoidal alluvial valleys with slope angles of 31^{o}, 45^{o}, and 71.5^{o}, which are located on bedrock with dimension of 2080x660 m. The depth of all valleys is 60 m and their bed length is 80 m. Given the reduced velocity of the shear waves of the surface layers relative to the bedrock in the most sites and also the experiences obtained from the previous earthquakes, only a vertical propagation angle is considered for the incident waves. Therefore, the velocity of shear wave is 200 m/s and 1000 m/s in alluvial valleys and bedrock, respectively. The alluvial basin and bedrock have elastic, dry, and homogeneous materials. Numerical models are identical in terms of layering and properties of layers' materials such as specific weight (γ), cohesion (C), angle of internal friction (φ), and Poisson's ratio (ν). The dimensions of the computational field and the location of the alluvial valley in the bedrock are selected so that, by creating a proper distance from the lateral boundaries of the model, the probable errors of reflection of waves after impacting on the boundaries are avoided. To this end, the lateral boundaries of the model are placed at a 2080 m distance from each other and are far enough away from the alluvial valley. Further, the bottom boundaries of the model are placed at a 600 m distance from the alluvial basin, which equals 10 times the depth of the valley.

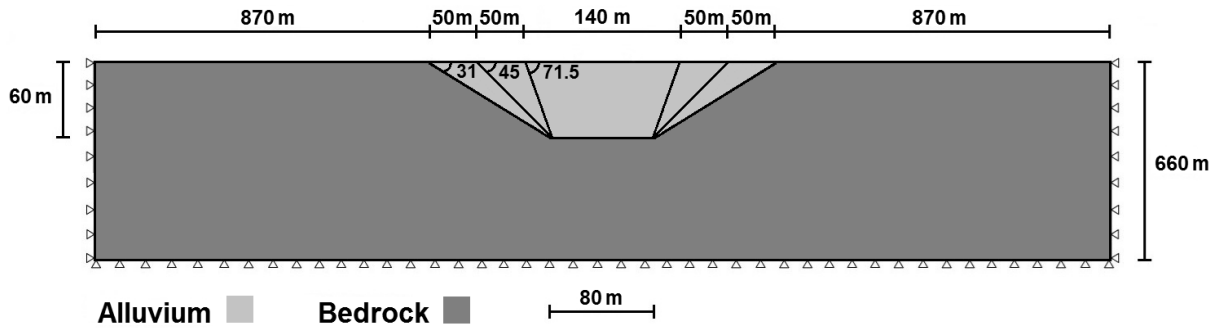

Fig. 1. Computational field, boundary conditions, and geometric dimensions of the numerical solution environment.

In order to study the effect of the slope angle of the valley on its seismic response, the impedance contrast (β) between the alluvial valley and the bedrock, which is defined as equation (1) (Le Pense et al., 2011), equals 0.135. Table 1 presents the mechanical properties of the materials used for numerical modeling of alluvial valleys and bedrock.

$$\beta = \frac{\rho_S C_S}{\rho_R C_R} \quad (1)$$

where ρ_S and ρ_R represent mass density of alluvium and bedrock, and C_S and C_R represent wave velocity in them, respectively.

Table 1. Geotechnical properties of materials.

Soil Type	γ (kN/m³)	ν	φ (deg)	C (kPa)	G_{max} (kPa)	V_s (m/s)	PI
Alluvium	18	0.3	34	30	7.2x104	200	30
Bedrock	26.5	0.4	44	233	26.5x106	1000	0

Figure 2 illustrates the variation of shear modulus ratio (G/G_{max}) with cyclic shear strain (γ_c). As can be seen, increasing the plasticity index (PI) in a constant cyclic shear strain leads to an increase in shear modulus ratio.

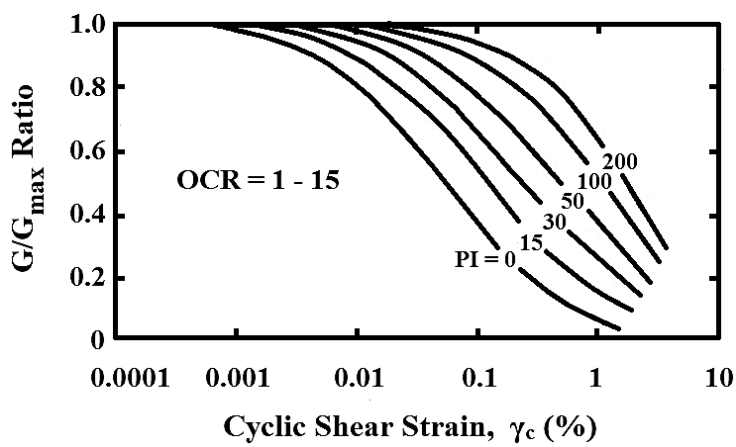

Fig. 2. Variation of shear modulus ratio (G/G_{max}) with cyclic shear strain (γ_c) (Kamatchi et al., 2013).

Figure 3 illustrates the variation of shear modulus ratio (G/G_{max}) with cyclic shear strain (γ_c) for alluvial valley and bedrock. These curves are prepared using QUAKE/W software.

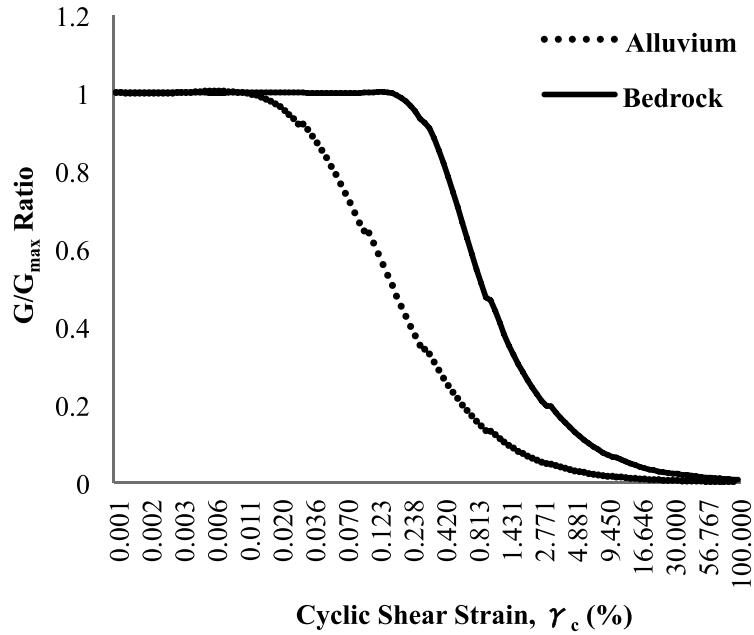

Fig. 3. Variation of shear modulus ratio (G/G_{max}) with cyclic shear strain (γ_c) for alluvial valley and bedrock.

Figure 4 illustrates the variation of damping ratio (D) with cyclic shear strain (γ_c). As can be seen, decreasing the plasticity index (PI) in a constant cyclic shear strain increases the damping ratio.

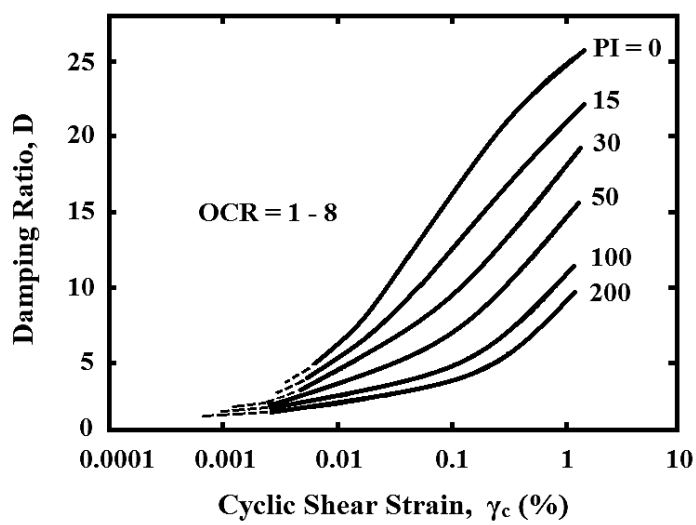

Fig. 4. Variation of damping ratio (D) with cyclic shear strain (γ_c). (Kamatchi et al., 2013).

Figure 5 illustrates the variation of damping ratio (D) with cyclic shear strain (γ_c) for alluvial valley and bedrock. These curves are prepared using QUAKE/W software. The damping ratio is determined using equation (2):

$$D = D_{\max}(1 - G/G_{max}) \quad (2)$$

where D represent damping ratio, D_{max} the maximum damping, and G/G_{max} the shear modulus ratio. Also, G_{max} is determined using equation (3) (Hammam and Eliwa, 2013):

$$G_{max} = \rho \, . \, V_s^2 \quad (3)$$

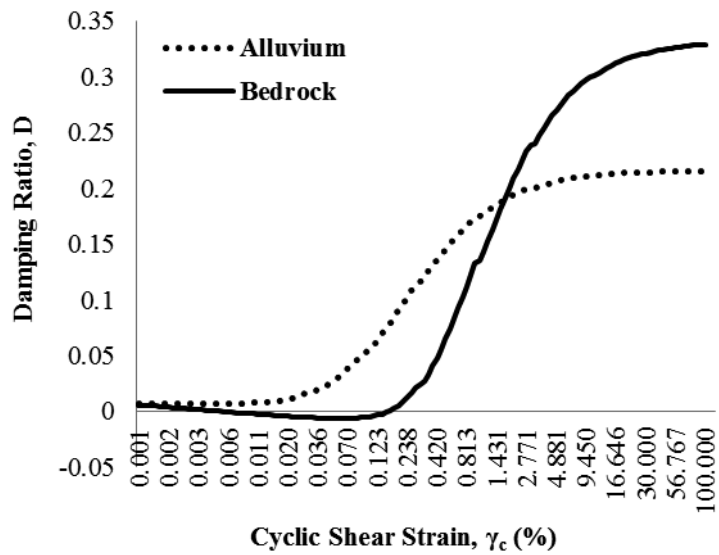

Fig. 5. Variation of damping ratio (D) with cyclic shear strain (γ_c) for alluvial valley and bedrock.

Meshing Size

The accuracy of numerical methods in solving dynamic problems requires selecting appropriate meshing sizes and a time interval proportional to the loading function. The selection of appropriate values for the mentioned parameters leads to optimization of model analysis time by the software, so that, in addition to increased accuracy of analysis and exact measurement of data, the time-consuming analysis is also avoided. Therefore before presenting the results, sensitization study, meshing size, time step length, and frequency content for incident waves are investigated. According to Figure 6, computational field, boundary conditions, and geometric dimensions of numerical solution environment are selected as identical in all models, and meshing size is selected as 5×5 m^2 squares. The boundaries around the computational field are selected as wave absorbing boundaries, so that after wave propagation and impacting on the sides of the model, they are not reflected and returned to the computational field. The number of nodes and elements of each model varies depending on the angle of slope of each valley, but these models have almost 52900 nodes and 52700 elements.

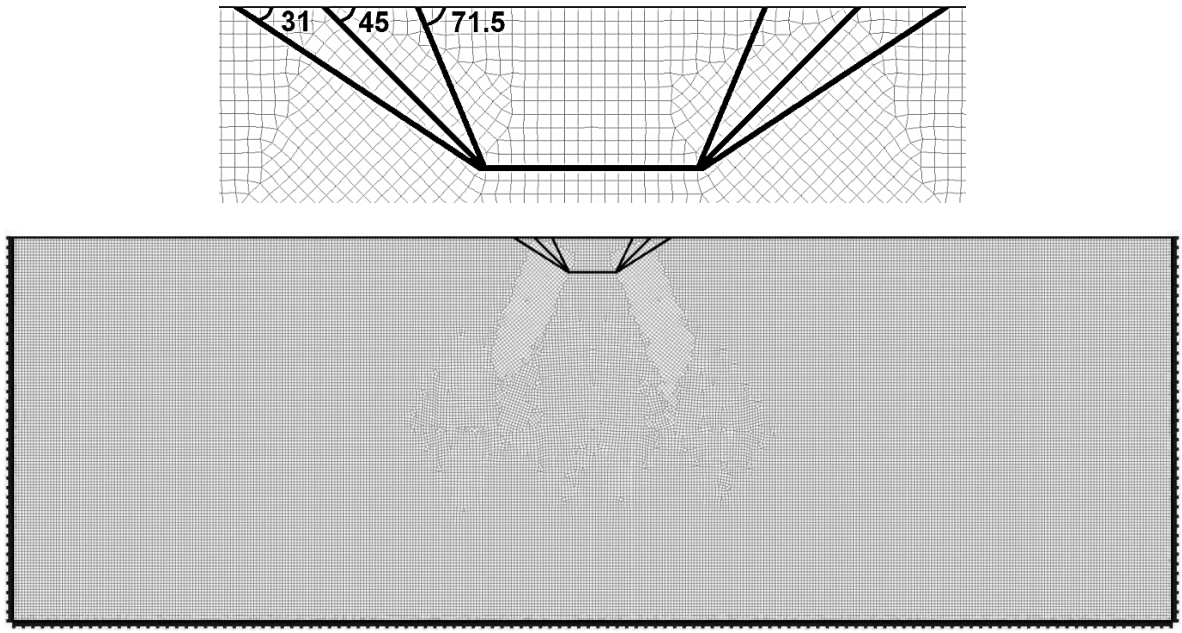

Fig. 6. Meshing dimensions of numerical solution environment.

Time Step

The number of time steps should be selected so that, in addition to fitting with meshing dimensions and enjoying proper precision to define incident wave length, it optimizes the duration of the analysis. In order to study the seismic response of trapezoidal alluvial valleys with different angles of slope, acceleration time-history of the El Centro earthquake with a maximum acceleration of 0.34 g and period of 10 sec was used, which is applied on bedrock in the form of P and SV vertically incident wave. In these situations, the peak acceleration and its maximum time are 341.7 cm/sec/sec and 2.14 sec, respectively. Figure 7 illustrates the acceleration time-history of the El Centro earthquake applied on the bedrock.

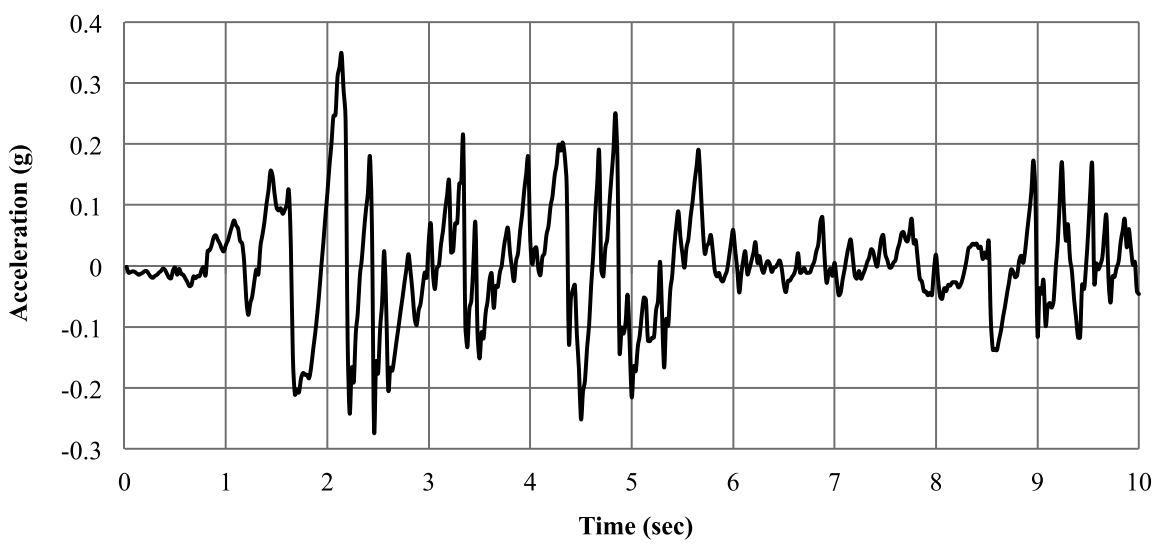

Fig. 7. Acceleration time-history of El Centro earthquake.

RESULTS AND DISCUSSION

Slope angle effect

Figure 8 illustrates the vertical displacement and acceleration curve of trapezoidal alluvial valleys with different angles of slope against the distance. Due to applying vertically incident waves, the maximum value of vertical displacement and acceleration occurs in the middle area of the valley with slope angle of 31° and increasing the slope angle of the valley decreases these values, so that the minimum value of vertical displacement and acceleration is observed in alluvial valley with a slope angle of 71.5°. Despite the different angles of slope of valleys in each model and consequently, different values of vertical displacement and acceleration, their incidence area is the same in all valleys, so that there is maximum value of displacement and acceleration in the middle area of valleys, compared to the adjacent area.

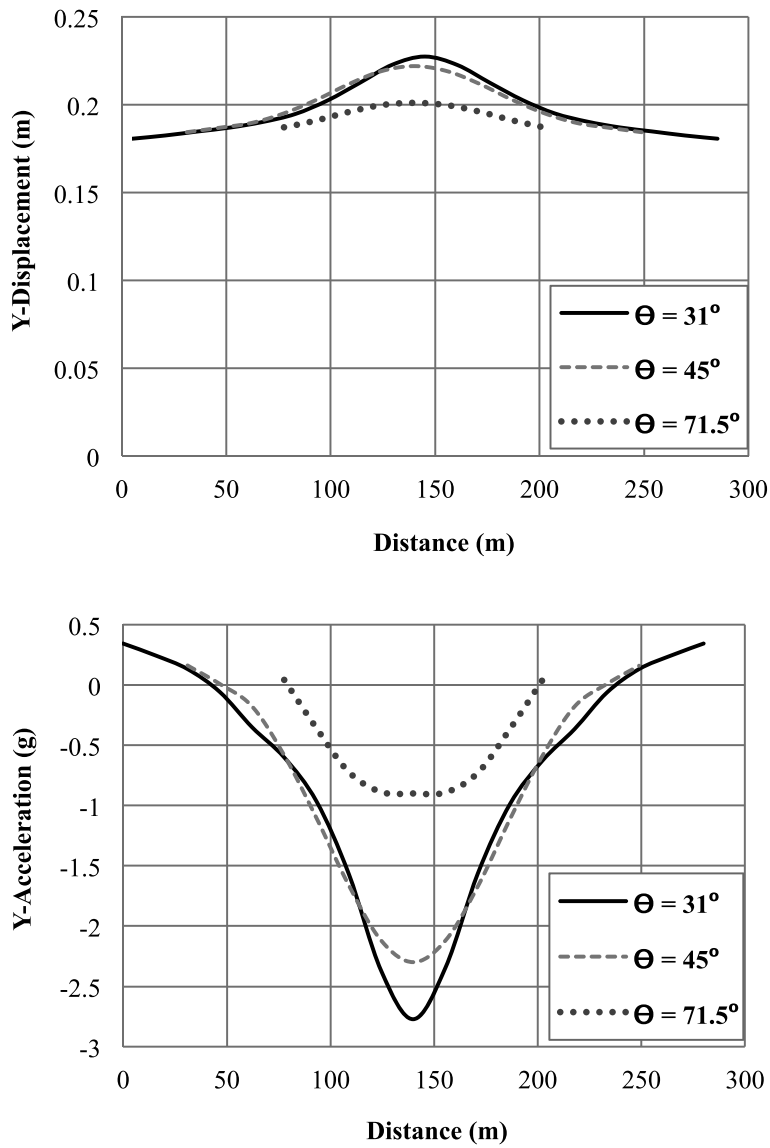

Fig. 8. Vertical displacement and acceleration curve of trapezoidal alluvial valleys with different angles of slope against the distance.

Response spectrum is one of the useful and important tools to recognize the earth movements and is widely used in earthquake engineering. In fact, the response spectrum explains the maximum response of the system against a particular input motion in the form of a function of the natural frequency and period, and damping coefficient of the system. In other words, the response spectrum illustrates the maximum response of different structures. Generally, amplitude, frequency content, and the duration of input motion are factors affecting spectral values. In all the modeled valleys, two relative maximum values in the middle and lateral areas of the valleys are observable and the magnification in the middle and lateral areas of the valley can be associated to sediments and topography effects, respectively. Figures 9 and 10 illustrate the vertical displacement response spectrum in the middle and lateral areas of trapezoidal alluvial valleys with different angles of slope. As can be observed, the maximum values of the vertical displacement response spectrum in the middle and lateral areas of the valleys are found in alluvial valleys with slope angles of 31^{o} and 71.5^{o}, respectively. Due to the sudden slope change, the sharp points of the phenomenon lead to an intense dispersion of incident waves. The trapezoidal valley with slope angle of 31^{o} has a larger area compared to other valleys, so this valley has larger dispersed waves amplitude and motion duration compared to them. By increasing the slope of the valley, the vertical displacement response spectrum in the middle and lateral areas of the valley decreases and increases, respectively. In fact, by increasing the slope angle of the valley, the maximum magnification value on the ground surface increases. Despite the decrease in vertical displacement response spectrum in the middle area and the slight increase in this spectrum in the lateral areas of the valley, the vertical displacement response spectrum is still higher in the middle area compared to the lateral areas. Therefore, regardless of the slope angle of the valley, the middle areas of the alluvial valleys generally have larger vertical displacement response spectrum compared to their lateral areas. Hence, in constant impedance, the lateral area of the valley has smaller magnification compared to its middle area. The main cause of wave amplification can be associated to the two factors of the increased amplitude of refracted waves relative to incident waves due to the hardness contrast between the two layers ($\beta \leq 3$ impedance ratio) and waves detention due to repeated reflections in the layers of sedimentary valley. In vertical propagation of the incident waves, increasing the slope angle of valley eliminates the possibility of waves' detention at valley's edges, and the magnification of the waves in the middle and corners of the valley increases and decreases, respectively. In fact, with the collision of shear waves to the corners of the valley (wave detention), Rayleigh surface waves are created on the surface of alluvial valley, which are propagated towards the middle area of the valley. Hence, alluvial valleys are affected by both effects of the topographic form and soil layers (the impedance between layers). If there is a large contrast between the layers (hardness difference), the surface waves move quickly between the edges and the corners of the valley and reflect, which leads to the increased magnification of the waves and vibration time (earth movement), compared to one-dimensional analysis. In this numerical modeling, the maximum values of the vertical displacement response spectrum in the middle and lateral areas of the alluvial valley are found in the period range of 0.3 to 0.5 sec, and this effect is reduced in higher periods. Moreover, by increasing the slope angle of the valley, the effect of Poisson's ratio increases and extends its domain of influence on magnification curve to range of larger periods.

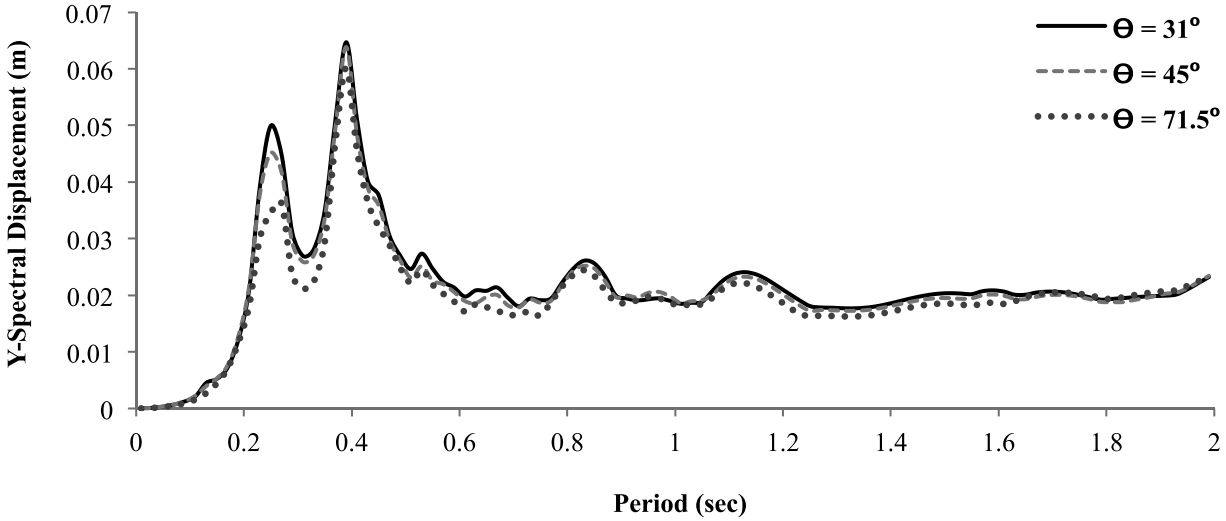

Fig. 9. Vertical displacement response spectrum in the middle area of trapezoidal alluvial valleys with different angles of slope.

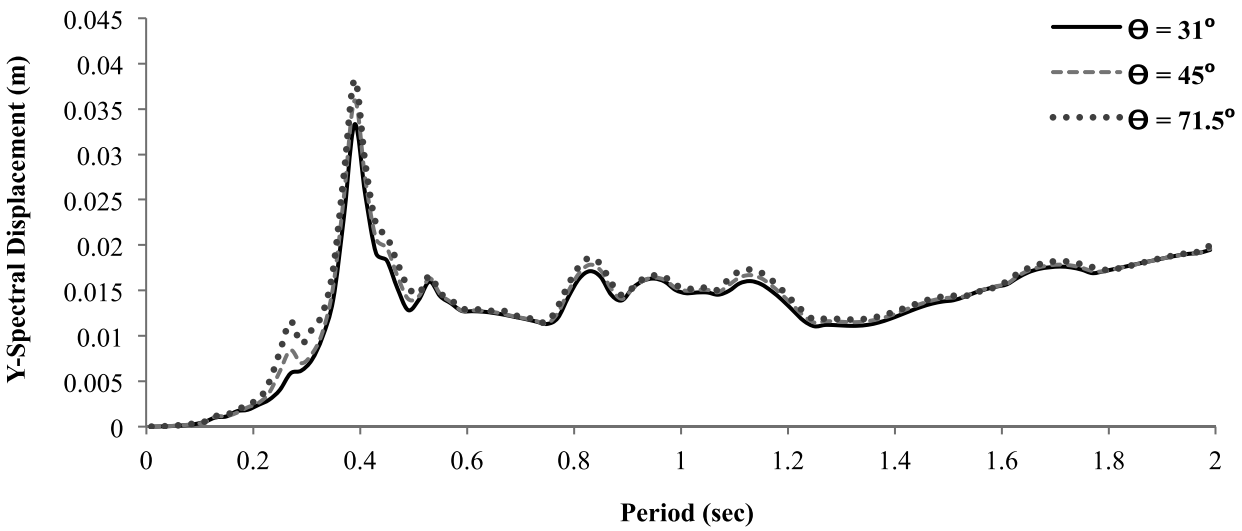

Fig. 10. Vertical displacement response spectrum in the lateral area of trapezoidal alluvial valleys with different angles of slope.

The vertical displacement response spectrum in the middle and lateral areas of trapezoidal alluvial valleys with different angles of slope is compared in Figure 11. As can be observed, in all models, the vertical displacement response spectrum is higher in the middle area of valleys compared to their lateral areas.

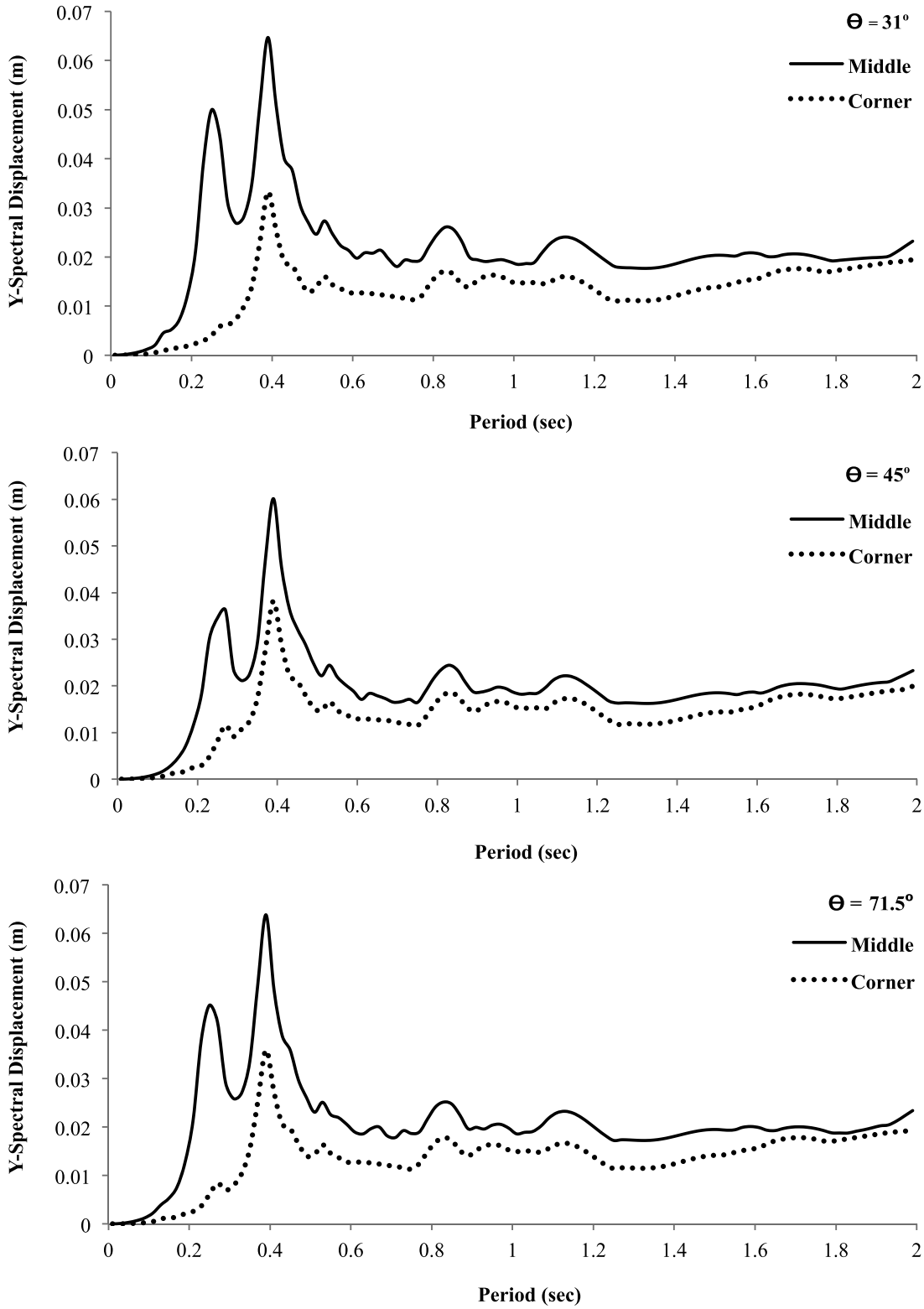

Fig. 11. Comparison of vertical displacement response spectrum in the middle and lateral areas of trapezoidal alluvial valleys with different angles of slope.

The acceleration response spectrum provides an estimate of the maximum acceleration at the bottom of the structure, relative to the natural period (T_n). Figures 12 and 13 illustrate the earthquake based vertical acceleration response spectrum in the middle and lateral areas of trapezoidal alluvial valleys with different angles of slope. The maximum values of vertical acceleration response spectrum in the middle and lateral areas of the valleys belong to alluvial valleys with slope angle of 31° and 71.5°, respectively. As was mentioned before, the larger the area of the valley, the larger its dispersed waves amplitude and the longer its movement time. Therefore, increasing the slope angle of the valley leads to decreases in the vertical acceleration response spectrum and increases in the middle and lateral areas of the valleys. Despite the vertical acceleration response spectrum reduction in the middle area of the valley and due to a slight increase in its value in the lateral areas, it has higher value in the center of the valley compared to its edges. Hence, regardless of the slope angle of the valley, the middle area of the alluvial valleys has generally higher vertical acceleration response spectrum compared to the lateral areas. In this numerical modeling, the maximum amount of vertical acceleration response spectrum in the middle and lateral areas of alluvial valleys is in the period range of 0.2 to 0.3 sec, and 0.3 to 0.4 sec respectively, which is reduced in both areas in higher periods.

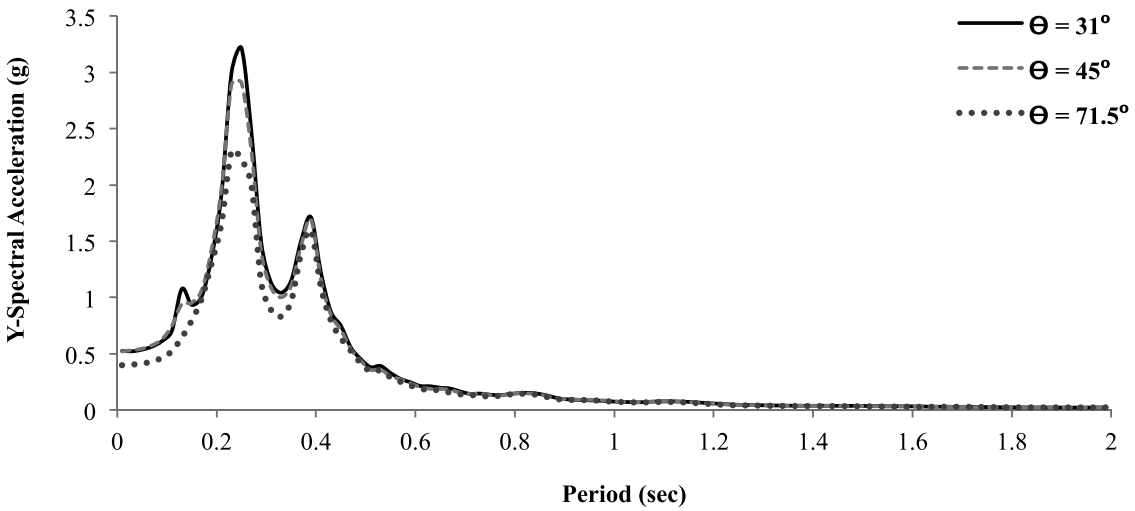

Fig. 12. Vertical acceleration response spectrum in the middle area of trapezoidal alluvial valleys with different angles of slope.

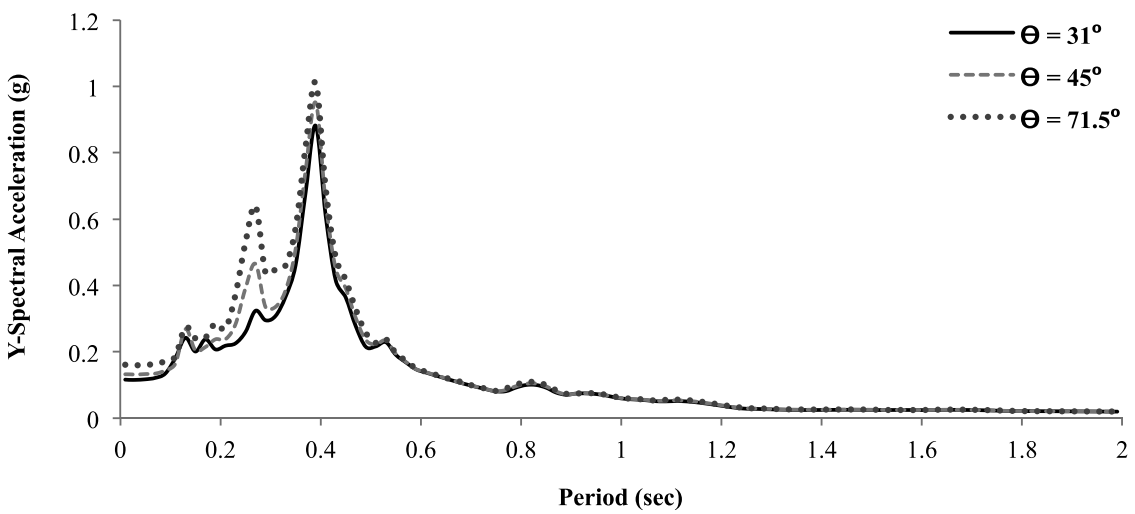

Fig. 13. Vertical acceleration response spectrum in the lateral area of trapezoidal alluvial valleys with different angles of slope.

Figure 14 illustrates the comparison of the vertical acceleration response spectrum in the middle and lateral areas of trapezoidal alluvial valleys with different angles of slope. As can be seen, in all models, the vertical acceleration response spectrum is higher in the middle area of valleys compared to their lateral areas.

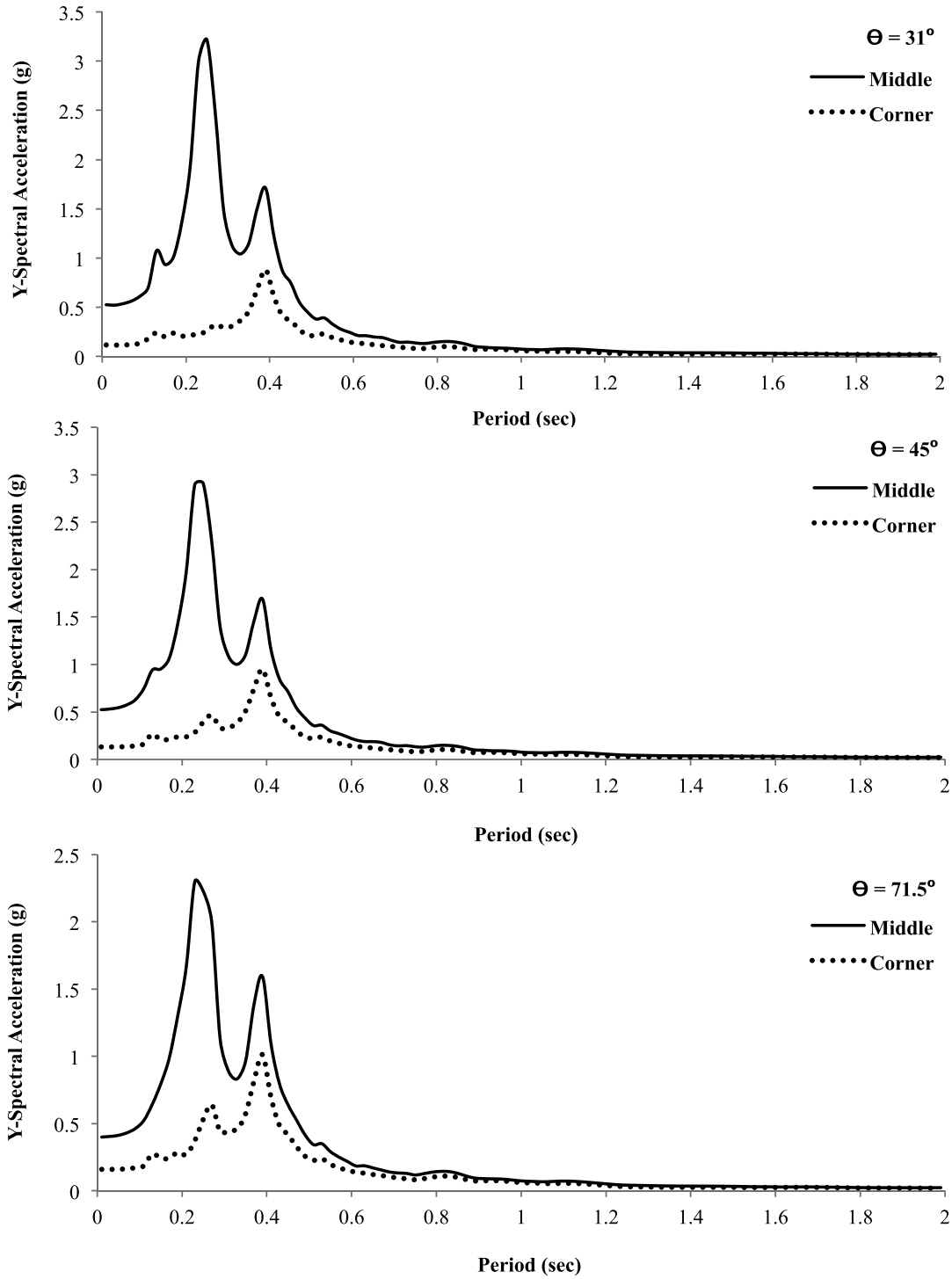

Fig. 14. Comparison of vertical acceleration response spectrum in the middle and lateral areas of trapezoidal alluvial valleys with different angles of slope.

Poisson's ratio effect

One of the most important factors influencing the seismic response of the alluvial valley against the incident waves is the Poisson's ratio of the basin. Four Poisson's ratios of 0.1, 0.2, 0.3, and 0.4 were considered for the alluvial deposits of trapezoidal valley with slope angle of 45° to investigate the effect of the Poisson's ratio of the alluvial basin on its seismic response against the vertically propagating incident waves in the present study. Other mechanical properties of the alluvial valley and bedrock are in accordance with Table 1 and Poisson's ratio of the bedrock is assumed to be 0.4.

Figures 15 and 16 illustrate the displacement time-history and displacement response spectrum variations in the middle and lateral areas of the alluvial valley with variation of Poisson's ratio, respectively. As can be observed, the severity of these variations is high in the middle area of the valley and intangible in the lateral areas. By decreasing the Poisson's ratio, the time-history and displacement response spectrum are increased in the middle area of the valley and are almost identical in the lateral areas. In this numerical modeling, the maximum values of the time-history and displacement response spectrum are found in the middle area of the alluvial valley with Poisson's ratio of 0.1, which are reduced by the increased Poisson's ratio, so that the minimum values of the time-history and displacement response spectrum belong to the middle area of alluvial valley with Poisson's ratio of 0.4. By approaching the lateral areas of the alluvial valley, the effect of Poisson's ratio on the time-history and displacement response spectrum variations of the valley is reduced, so that the variation in the Poisson's ratio of the alluvial sediments has intangible effect on the time-history and displacement response spectrum of the lateral areas of the valley.

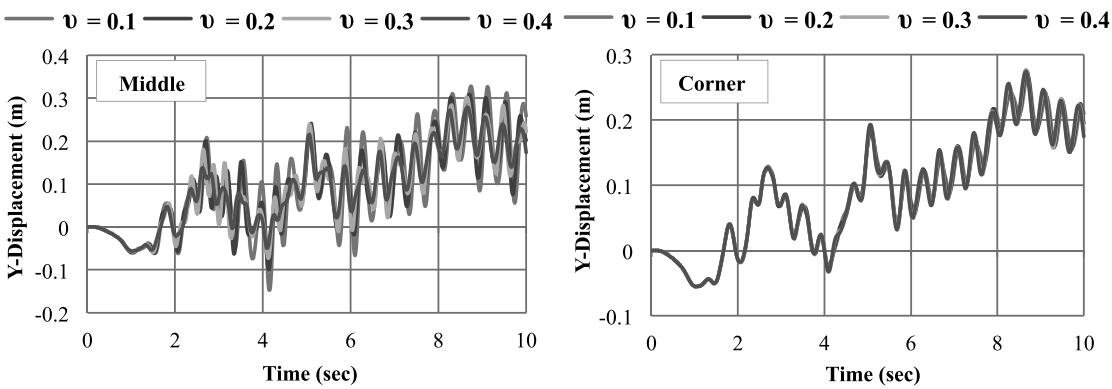

Fig. 15. Displacement time-history in the middle and lateral areas of the alluvial valley with variation of Poisson's ratio.

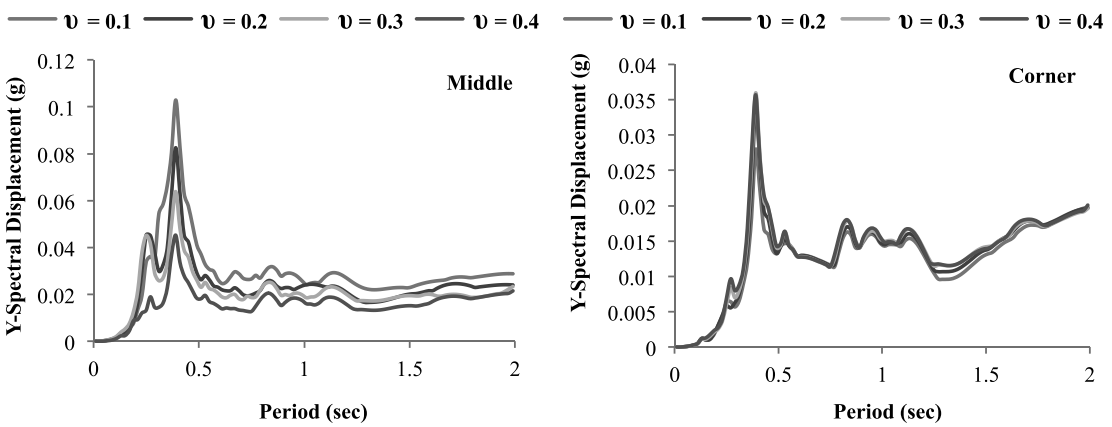

Fig. 16. Displacement response spectrum in the middle and lateral areas of the alluvial valley with variation of Poisson's ratio.

Figures 17 and 18 present the acceleration time-history and acceleration response spectrum variations in the middle and lateral areas of the alluvial valley with variation of Poisson's ratio, respectively. As can be observed, these variations are more severe in the middle area and intangible in the lateral areas of the valley. Reducing the Poisson's ratio increases the time-history and acceleration response spectrum in the middle area of the valley, while they have intangible effects in the lateral areas of the valley. In this numerical modeling, the maximum values of the time-history and acceleration response spectrum are found in the middle area of the alluvial valley with Poisson's ratio of 0.1, which are reduced by the increased Poisson's ratio, so that the minimum values of the time-history and acceleration response spectrum belong to the middle area of alluvial valley with Poisson's ratio of 0.4. By approaching the lateral areas of the alluvial valley, the impact of Poisson's ratio on the time-history and acceleration response spectrum variation of the valley is reduced, so that the variation in the Poisson's ratio of the alluvial sediments has intangible effect on the time-history and acceleration response spectrum of the lateral areas of the valley.

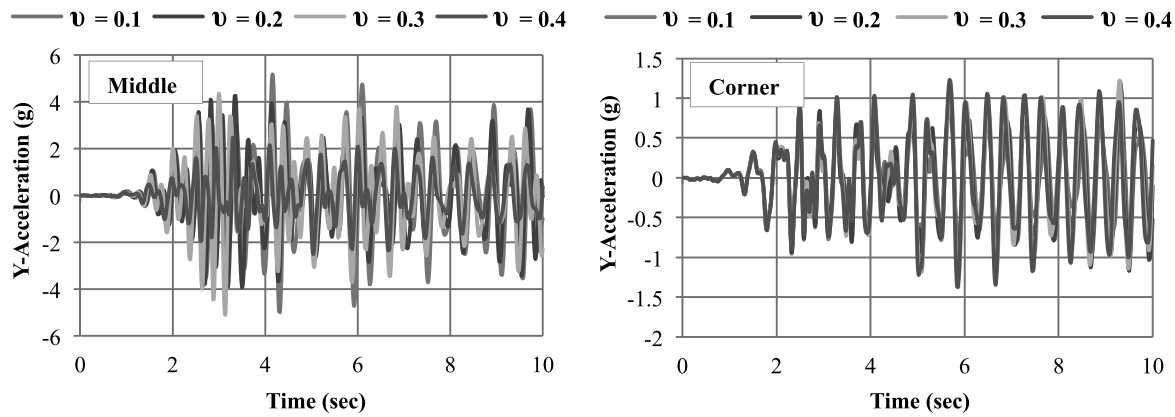

Fig. 17. Acceleration time-history in the middle and lateral areas of the alluvial valley with variation of Poisson's ratio.

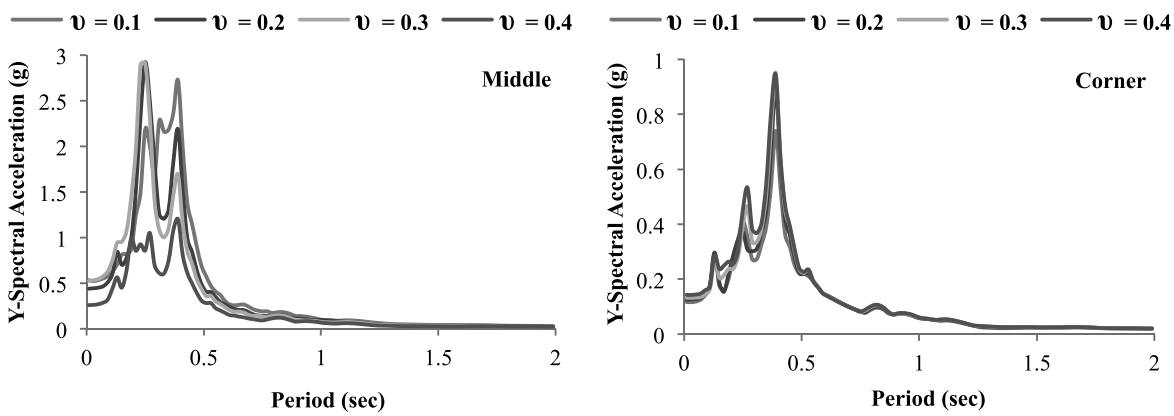

Fig. 18. Acceleration response spectrum in the middle and lateral areas of the alluvial valley with variation of Poisson's ratio.

Specific weight effect

The soil amplification effects are usually larger than the topographic amplification effects within the alluvial valley, while the topographic effects dominate the amplification pattern of ground motions outside the alluvial valley (Zhang et al., 2017). As was mentioned before, magnification in the middle and lateral areas of the valleys is due to sediments and topographic effects, respectively. Therefore, one of the most important factors affecting the seismic

response of the alluvial valley against the incident waves is the material properties of the basin. Four specific weights of 14, 16, 18, and 20 kN/m^3 were considered for the alluvial sediments of the trapezoidal valley with slope angle of 45^o to examine the effect of the alluvial sediments on the seismic response of the valley against vertically propagating incident waves in the present study. Other mechanical properties of the alluvial valley and bedrock are according to Table 1, and the specific weight of the bedrock is assumed to be 26.5 kN/m^3.

Figures 19 and 20 illustrate the displacement time-history and displacement response spectrum variation in the middle and lateral areas of the alluvial valley, respectively. Comparing the displacement time-history does not reveal a significant difference in its values in each middle and lateral area of the valley. However, there is higher disturbance and turbulence in the displacement time-history of middle area of the valley compared to its lateral areas. In this numerical modeling, the maximum values of the displacement response spectrum are found in the middle area of the alluvial valley with specific weight of 20 kN/m^3 , which are reduced by the increased specific weight. According to equation (1), variation in the specific weight of the materials results in a variation in the impedance ratio (β) between the alluvial valley and bedrock. Increasing the density of the alluvial sediments (ρ_S), and constant bedrock density (ρ_R) and wave velocity in alluvial layers (C_S) and bedrock (C_R), results in an increase in the impedance ratio (β) between the alluvial valley and bedrock. Increasing the impedance or material hardness on the alluvial valley leads to an increase displacement response spectrum in its middle area and by approaching to its lateral areas, the impedance effect on displacement response spectrum of valley is reduced, so that variation in the specific weight of the alluvial sediments has intangible effect on displacement response spectrum in the lateral areas of the valley. Reduced hardness of sediments can lead to a reduction in the topographic effect in the lateral areas of the valley, so that in the very soft sediments the effect of material impedance is dominant and the maximum magnification is found in the middle area of the valley.

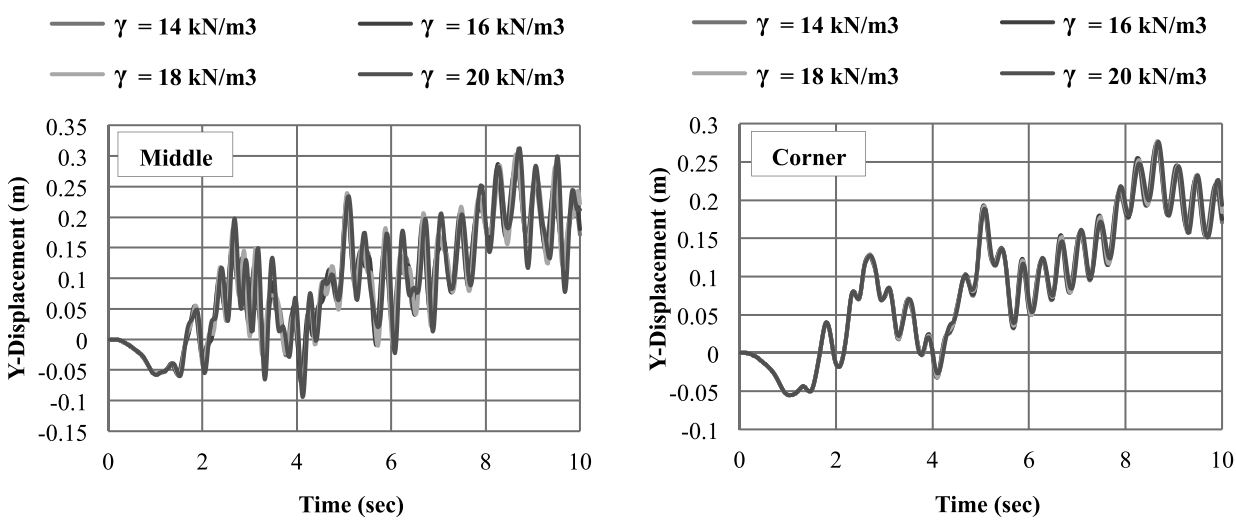

Fig. 19. Displacement time-history in the middle and lateral areas of the alluvial valley with variation of specific weight.

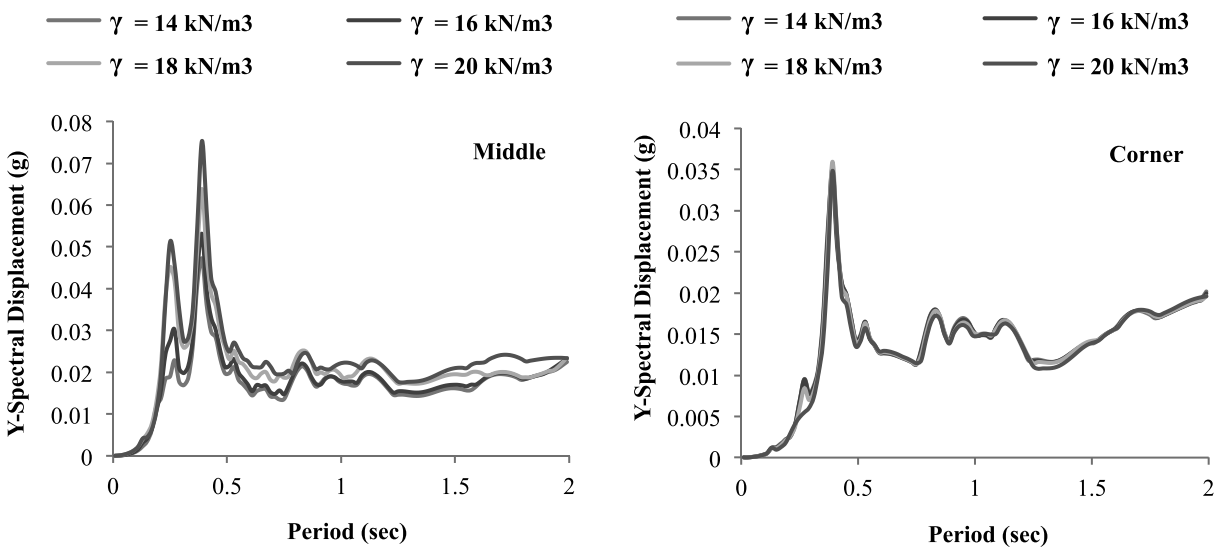

Fig. 20. Displacement response spectrum in the middle and lateral areas of the alluvial valley with variation of specific weight.

Figures 21 and 22 illustrate acceleration time-history and acceleration response spectrum variation in the middle and lateral areas of the alluvial valley, respectively. As can be seen, variation in the specific weight of the alluvial sediments changes the impedance of the valley and leads to variation in the impedance ratio (β) between the alluvium and bedrock. Therefore, there is turbulence and disturbance in the acceleration time-history of the middle and lateral areas of the valley; however, comparing the acceleration time-history variations caused by various impedances does not reveal a significant difference in acceleration time-history values in middle and lateral areas of the valley. Increasing the specific weight of alluvial mat erials leads to a slight change in the acceleration response spectrum values in the middle and lateral areas of the valley, respectively. Therefore, in this numerical modeling, the maximum values of acceleration response spectrum are found in the middle area of the alluvial valley with specific weight of 20 kN/m^3, and reduction in the specific weight of the materials of the valley reduces the acceleration response spectrum value in the mentioned area. In fact, reducing the specific weight of the material of the alluvial valley results in a reduction in the impedance or material hardness and accordingly, reduction in the acceleration response spectrum in the middle area of the valley. By approaching the lateral areas of the alluvial valley, the effect of impedance on acceleration response spectrum variations of the valley is reduced, so that variation in the specific weight of the alluvial sediments has intangible effect on the acceleration response spectrum in the lateral areas of the valley. In fact, increasing the impedance ratio between the two layers of alluvium and bedrock leads to increasing the response spectrum of the valley.

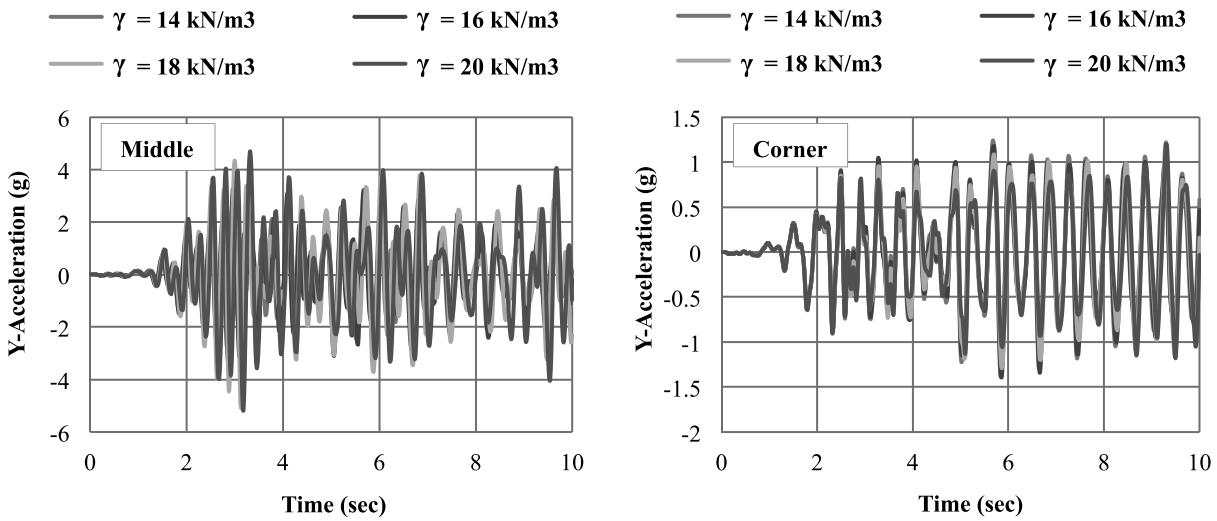

Fig. 21. Acceleration time-history in the middle and lateral areas of the alluvial valley with variation of specific weight.

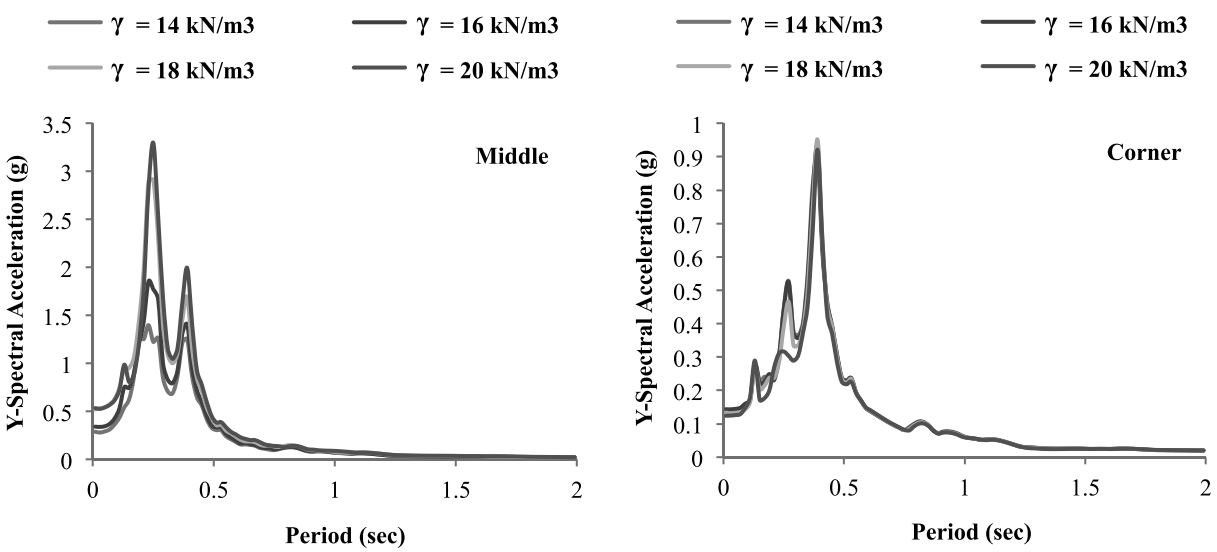

Fig. 22. Acceleration response spectrum in the middle and lateral areas of the alluvial valley with variation of specific weight.

CONCLUSION

Using numerical modeling of 2D trapezoidal alluvial valleys located on bedrock and with slope angles of 31°, 45°, and 71.5°, the present study investigated their seismic response against P and SV vertically propagating incident waves. The numerical simulation was performed using QUAKE/W finite element software, based on linear equation analysis. According to the results, due to a sudden slope variation, the sharp points of the phenomenon lead to an intense dispersion of incident waves. The trapezoidal valley with smaller slope angle and larger area has larger dispersed waves amplitude and longer movement time compared to other valleys with larger slope angles. In vertical propagation of incident waves, the increased slope angle of the valley eliminates the possibility of waves' detention

at valley's edges, and there is a smaller wave magnification in the corners of the valley and higher magnification in its middle area. In addition, the increased slope angle of the valley results in a decrease and increase in the vertical displacement and acceleration response spectrum in the middle and lateral areas of the valleys, respectively. Despite the vertical displacement and acceleration response spectrum reduction in the middle area of the valley and due to a slight increase in their values in the lateral areas, they still have greater values in the center of the valley compared to its edges. Comparing four Poisson's ratios of 0.1, 0.2, 0.3, and 0.4 and four specific weights of 14, 16, 18, and 20 kN/m^3 of the alluvial sediments revealed that increasing Poisson's ratio reduces the displacement and acceleration response spectrum in the middle area of the valley, but does not have tangible effects in its lateral areas. Further, increasing the specific weight of alluvial materials leads to an increase in impedance of the alluvial valley and accordingly, increased displacement response spectrum in the middle area of the valley. By approaching the lateral areas of the alluvial valley, the impedance influence on the displacement response spectrum variations of the valley is reduced, so that the variation in the specific weight of alluvial sediments has intangible effect on the displacement response spectrum of the lateral areas of the valley.

ACKNOWLEDGMENT

The authors warmly appreciate the cooperation and guidance of Dr. H. Alielahi in this study.

REFERENCES

Bararpour, M., Janalizade, A. & Tavakoli, H.R. 2016. The effect of 2D slope and valley on seismic site response. Arabian Journal of Geosciences, **9**(93): 1-10.

Benioff, H. 1955. Mechanism and strain characteristics of the white wolf fault as indicated by aftershocks sequence. Calif. Div. Mines Bull, **171**: 199-202.

Bouchon, M. 1973. Effect of Topography on Surface Motion. Bull. Bulletin of the Seismological Society of America, **63**: 615-632.

Geli, L., Bard, P.V. & Julien, B. 1988. The Effect of Topography on Earthquake Ground Motion: A Review and New Results. Bulletin of the Seismological Society of America, **78**(1): 42-63.

Hammam, A.H. & Eliwa, M. 2013. Comparison between results of dynamic & static moduli of soil determined by different methods. HBRC Journal, **9**(2): 144–149.

Kamalian, M., Jafari, M.K., Razmkhah, A. & Sohrabi-Bidar, A. 2004. Amplification Pattern of 2D Semi-Elliptical Shaped Hills Subjected To Vertically Propagating Incident Waves. AmirKabir Engineering Journal. (In Persian)

Kamalian, M., Jafari, M.K., Sohrabi-Bidar, A. & Razmkhah, A. 2004. Amplification Pattern of 2D Trapezoidal Shaped Hills Subjected To Vertically Propagating Incident Waves. Tarbiat Modares Engineering Journal. (In Persian)

Kamalian, M., Jafari, M.K., Sohrabi-Bidar, A. & Razmkhah, A. 2008. Seismic Response of 2-D Semi-Sine Shaped Hills to Vertically Propagating Incident Waves: Amplification Patterns and Engineering Applications. Earthquake Spectra Journal, **24**(2): 405-430.

Kamatchi, P., Ramana, G.V., Nagpal, A.K. & Iyer, N.R. 2013. Modelling Propagation of Stress Waves through Soil Medium for Ground Response Analysis. Journal of Engineering, **5**: 611-621.

Le Pense, S., Gatmiri, B. & Maghoul, P. 2011. Influence of soil properties and geometrical characteristics of sediment-filled valleys on earthquake response spectra. 8th International Conference on Structural Dynamics, pp.130-136.

Moczo, P., Bystricky, E., Kristek, J., Carcione J.M. & Bouchon, M. 1997. Hybrid Modeling of P-SV Seismic Motion at Inhomogeneous Viscoelastic Topographic Structures. Bulletin of the Seismological Society of America, **87**(5): 1305-1323.

Pedersen, H.A., Sanchez-Sesma, F.J. & Campillo, M. 1994. Three-Dimensional Scattering by Two-Dimensional Topographies. Bulletin of the Seismological Society of America, **84**(4): 1169-1183.

QUAKE/W. Finite Element Dynamic Earthquake Analysis Software, Geo-Slope Office, 2012.

Sánchez-Sesma, F.J. & Campillo, M. 1991. Diffraction of P, SV and Rayleigh Waves by Topographic Features: A Boundary Integral Formulation. Bulletin of the Seismological Society of America, **81**(6): 2234-2253.

Sánchez-Sesma, F.J. & Campillo, M. 1993. Topographic Effects for Incident P, SV and Rayleigh Waves. Tectonophysics, **218**: 113-125.

Sánchez-Sesma, F.J. 1987. Site Effects on Strong Ground Motion. Soil Dynamics and Earthquake Engineering, **6**(2): 124-132.

Zhang, N., Gao, Y. & Dai, D. 2017. Ground Motion at a Semi-Cylindrical Valley Partially Filled with a Crescent-Shaped Soil Layer Under Incident Plane SH Waves. Journal of Earthquake and Tsunami, **11**(1): 13–26.

Submitted: 08/06/2017
Revised: 26/09/2017
Accepted: 10/10/2017

دراسة عددية للاستجابة الزلزالية للوديان الغرينية شبه المنحرفة ضد الموجات العامودية المهاجمه

محمد حسين تقى زاده ولدى، **محمد رضا عطرشيان، ***عطا جعفرى شالكوهى و*على تيغ نورد بلسبنه**

*قسم الهندسة المدنية، فرع اصفهان (خوراسغان)، جامعة آزاد الإسلامية، اصفهان، إيران

**قسم الهندسة المدنية، فرع زنجان، جامعة آزاد الإسلامية، زنجان، إيران

***قسم الهندسة المدنية، فرع بندر أنزلي، جامعة آزاد الإسلامية، بندر أنزلي، إيران

****قسم الهياكل والمواد، كلية الهندسة المدنية، جامعة التكنولوجيا ماليزيا، ماليزيا

الخلاصة

تشير الزلال المتكررة في العالم إلى أن الأضرار الهيكلية الناتجة عن الزلال، تتأثر بشكل كبير بحالة الموقع، وهو ما يسمى بتأثيرات الموقع. والسبب في ذلك يعود إلى أن غالبية المدن قد شيدت على تربة غرينية ولذلك فإن دراسة الاستجابة الزلزالية للأحواض الغرينية والتي هي موقع العديد من الهياكل، أمر في غاية الأهمية. في هذه الدراسة ستتم الاستفادة من النمذجة العددية للوديان الغرينية شبه المنحرفة ثنائية الأبعاد بزوايا انحدار 31 و45 و71.5 درجة على أساس حجري، واستجاباتها الزلزالية ضد الموجات العامودية الهاجمة P وSV، في منطقتين وسطى وجانبية من الوادي. ثم ستتم دراسة تأثير التغيرات في نسبة بواسون والوزن النوعي للمواد الغرينية على أساس الاستجابة الزلزالية للوادي في المناطق المذكورة. تتم النمذجة العددية باستخدام برنامج طريقة العناصر المحددة QUAKE/W بناءً على تحليل التكافؤ الخطي. تشير النتائج إلى أنه مع زيادة زاوية انحدار الوادي، ينخفض نطاق استجابة تغيير المكان والتسارع العامودي الناتج عن الزلزال في المنطقة الوسطى من الوادي الغريني، بينما يزداد في المنطقة الجانبية منه. علاوة على ذلك، فمع زيادة نسبة بواسون والوزن النوعي للمواد الغرينية، ينخفض نطاق استجابة تغيير المكان والتسارع العامودي في المنطقة الوسطى من الوادي، أما في المناطق الجانبية منه، فإن تغييرات نطاق الاستجابة بشأن تغيير المكان والتسارع العامودي لا يخضع لتغيرات ملموسة.